Applied Physics Letters

Magneto-ionic enhancement and control of perpendicular magnetic anisotropy

Cite as: Appl. Phys. Lett. **121**, 222402 (2022); https://doi.org/10.1063/5.0121767
Submitted: 19 August 2022 • Accepted: 31 October 2022 • Published Online: 29 November 2022

Alexander E. Kossak, Daniel Wolf and Geoffrey S. D. Beach

COLLECTIONS

Note: This paper is part of the APL Special Collection on Magneto-ionic and electrostatic gating of magnetism: phenomena and devices.

This paper was selected as an Editor's Pick

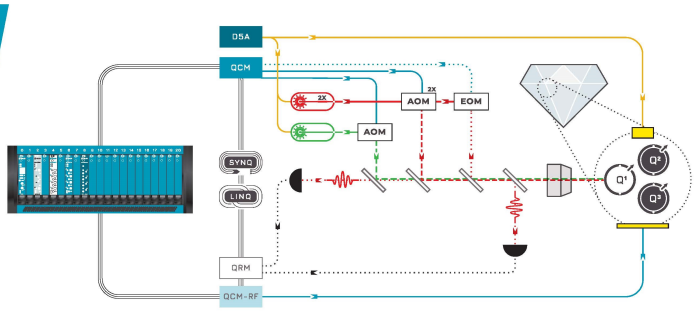

Applied Physics Letters ARTICLE scitation.org/journal/apl

Magneto-ionic enhancement and control of perpendicular magnetic anisotropy

Cite as: Appl. Phys. Lett. **121**, 222402 (2022); doi: 10.1063/5.0121767
Submitted: 19 August 2022 · Accepted: 31 October 2022 ·
Published Online: 29 November 2022

Alexander E. Kossak,[1,a)] Daniel Wolf,[2] and Geoffrey S. D. Beach[1]

AFFILIATIONS

[1]Department of Materials Science and Engineering, Massachusetts Institute of Technology, Cambridge, Massachusetts 02139, USA
[2]Leibniz Institute for Solid State and Materials Research Dresden, Helmholtzstraße 20, 01069 Dresden, Germany

Note: This paper is part of the APL Special Collection on Magneto-ionic and electrostatic gating of magnetism: phenomena and devices.
[a)]**Author to whom correspondence should be addressed:** akossak@mit.edu

ABSTRACT

Magneto-ionic control of magnetic anisotropy is an emerging voltage-controlled approach that aims to offer much lower power consumption than current-controlled manipulation of magnetization. Moreover, magneto-ionic systems are ideal candidates for non von Neumann computing architectures, such as neuromorphic and stochastic computing due to their non-volatile and analog nature. One of the key metrics to quantify the efficiency of voltage-controlled magnetic anisotropy (VCMA) is the magneto-electric voltage coefficient ($\Delta H_c/|\Delta V|$). Here, we show greater than one order of magnitude improvement in this efficiency compared to existing solid-state systems using a Co/Pd multilayer heterostructure. By performing a systematic study of the Co thickness, the Pd thickness, and the number of repeat units of engineered Co/Pd multilayers, we identify a narrow bandwidth of the Co thickness from 2–2.5 Å, Pd thickness from 1.4–1.7 nm, and repeat units from 7–9, to maximize the VCMA. Compared to rivaled liquid electrolyte systems, this platform has the advantage of faster speeds and easier integration for on-chip logic and memory devices.

As the limits of complementary metal-oxide semiconductor technology are being reached, spin-based devices are being deployed to reduce power consumption and scale.[1] The primary logic operation is the switching of the magnetization of one or more magnetic layers. This has typically been done using magnetic fields generated by currents, spin-polarized current-induced spin transfer torques (STT), or spin-orbit torques (SOT).[2,3] However, the high current densities and undesirable Joule heating lead to high energy consumption and challenges with heat dissipation. Using an electric field to control magnetization has arisen as a promising alternative for on-chip devices due to its low-power consumption, reversibility, speed, and non-volatility.[4–7] Magneto-ionic gating is an emerging voltage-controlled approach that aims to both electrically control and offer substantial modulation of several magnetic interactions and material properties.[8,9] Hydrogen based devices, as opposed to oxygen,[8–12] have shown the ability to modulate magnetic properties at higher speeds and over more cycles than any other ion without causing structural degradation.[13]

Magneto-ionic systems are ideal candidates for non von Neumann architectures due to their low power, non-volatile, and analog nature. Scaling current generation devices down would push power consumption down to 1–10 aJ/bit.[14,15] Moreover, the continuous changes in magnetic properties, such as saturation magnetization and coercivity, allow for voltage-dependent learning processes that are desired in stochastic or neuromorphic architectures, magnetic random access memory, and logic devices.[16,17]

The experiments herein used a multilayer heterostructure consisting of Ta(3.5)/Pt(5)/Co(X)/[Pd(Y)/Co(X)]$_N$/Pd(6)/GdO_x(26)/Au(8) (thickness in nm) where the Co thickness (X), Pd thickness (Y), and number of repeating units (N) were systematically explored from 0.1–0.35 Å, 0.6–3.45 nm, and 3–11 repeat units, respectively. All of the samples were grown using DC magnetron sputtering at room temperature and a background pressure $<1 \times 10^{-7}$ Torr on 50 nm wet thermally oxidized silicon (100) substrates. Au was grown under 3.5 mTorr Ar while the rest of the metal layers were grown under 3 mTorr Ar. The GdO_x layer was deposited using radio-frequency sputtering with 3 mTorr Ar and 0.7 mTorr O_2. Shadow masking was used to pattern circular Au electrodes on top of the GdO_x with an approximate diameter of

100 μm while the continuous bottom metal layer served as the counter electrode.

The heterostructure is schematically shown in Fig. 1(a). In the virgin state, all films exhibited perpendicular magnetic anisotropy (PMA) measured via polar magneto-optical Kerr effect (MOKE) microscopy. The voltage-controlled hydrogen (H) gating of these films was studied using the solid-state proton pump platform introduced in Ref. 9 and used to gate Pd/Co/Pd trilayers. Exemplary hysteresis loops for a $[Pd(1.5)/Co(0.25)]_5$ heterostructure are shown in Fig. 1(b). In the ungated virgin state (black line), the square out-of-plane (OOP) hysteresis loop indicates PMA while under a positive gate voltage (V_g) = +4 V (purple line), H is sourced from atmospheric H_2O split at the Au/ambient interface,[18] loaded into the heterostructure, and leads to in-plane (IP) anisotropy as evidenced by the flat OOP hysteresis loop. When a negative V_g is subsequently applied, H is unloaded from the system, and PMA returns. However, unlike the trilayer system studied in Ref. 9, during the first few gating cycles, the coercivity of the H-unloaded state progressively increases in an irreversible fashion, and only after several cycles does the coercivity of the unloaded state stabilize. This is seen in Fig. 1(b), where for each cycle V_g was applied for 30 s at +4 V followed by -1 V for 30 s. The application of higher negative biases does not allow for the recovery of the virgin state. After several cycles, the coercivity of the unloaded state begins to saturate, while still allowing the anisotropy to be toggled from OOP to IP by H loading/unloading reversibly, as seen in Fig. S1.

Irreversible coercivity enhancement due to magneto-ionic gating has previously been seen in exchange-biased Pd/Co/Pd tilayers.[11] The irreversible change in that study was attributed to a phase transformation of the Co from an amorphous to a crystalline state—revealed by cross-sectional high resolution transmission electron microscopy (HR-TEM). However, cross-sectional HR-TEM for a $[Co(0.2)/Pd(2)]_{11}$ multilayer heterostructure in this study shows no discernible change in the structure of the magnetic multilayers between its virgin state [Fig. 1(c)] and after several gating cycles [Fig. 1(d)]. In fact, in the virgin state, the Co/Pd multilayer is already crystalline, as seen in Fig. S2(a). Modification of the coercivity in Co/Pd multilayers has also been seen in studies using gaseous H exposure.[19–22] However, these studies have conflicting results. The hydrogen increases the coercivity for some and decreases for others. Moreover, the mechanism by which the coercivity changes is claimed to be structural in some studies and electronic in others. A recent study using density functional theory provided some insight into the previous contradicting results.[23] It was shown that small amounts of H that enter the bulk of the thin film can enhance the PMA while larger amounts at the interface will reduce the

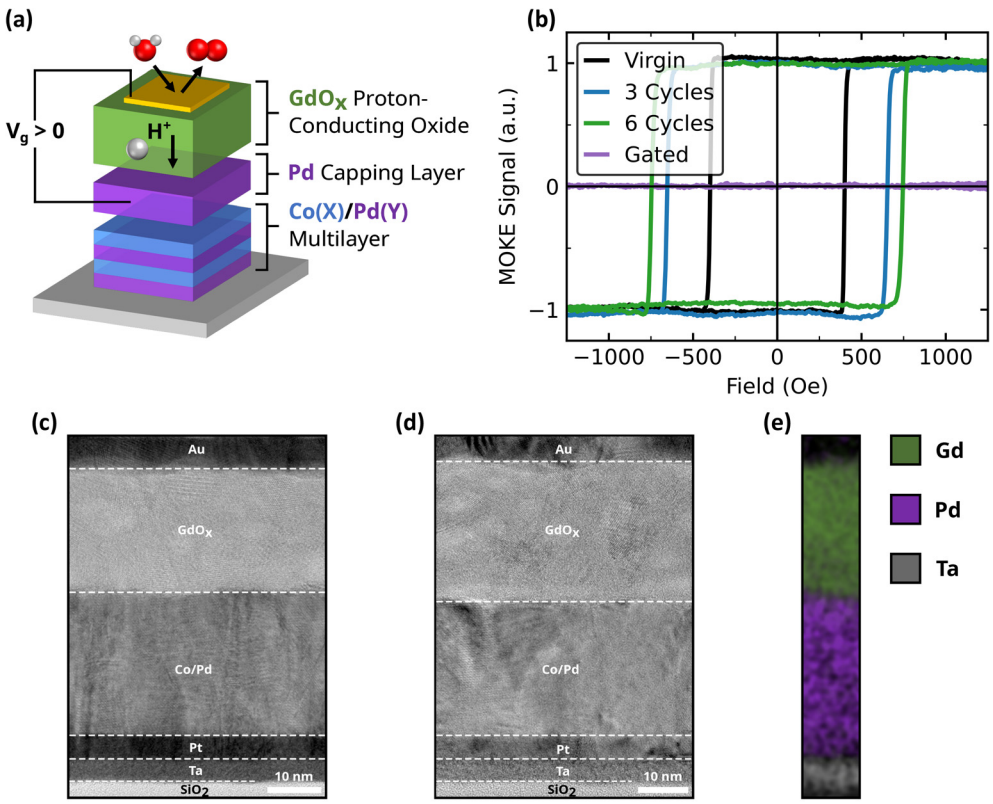

FIG. 1. Co/Pd multilayers. (a) Illustrative schematic of the multilayer heterostructure made of Ta(3.5)/Pt(5)/Co(X)/$[Pd(Y)/Co(X)]_N$/Pd(6)/GdO_x(26)/Au(8) and deposited using magnetron sputtering. (b) Polar MOKE hysteresis loops of a $[Pd(1.5)/Co(0.25)]_5$ heterostructure in the ungated virgin state (black), in the H-unloaded state after three cycles (blue), after six cycles (green), and in the H-loaded state (purple). (c), Cross-sectional high-resolution transmission electron micrographs of the $[Co(0.2)/Pd(2)]_{11}$ heterostructure in the ungated virgin state and (d) after several gating cycles. (e) Qualitative elemental map slice (color-coded) obtained by energy-loss filtered transmission electron microscopy.

PMA. The enhancement of PMA can be attributed to a modification of the structural properties, such as the formation of a β-Pd-H phase and subsequent lattice expansion.[19] By contrast, the reduction of PMA can be attributed to a modification of the electronic properties, namely, the hybridization between 4*d* Pd orbitals and 3*d* Co orbitals.[23,24] These two possible contributions would lead to a non-monotonic and potentially competing modification of the Co/Pd multilayer coercivity under H loading.

One possible structural transformation of the Co/Pd multilayer that could lead to an irreversible increase in coercivity is the H-induced phase transformation of α-Pd-H to β-Pd-H. This would be accompanied by an increase in the d_{111} spacing by approximately 4%–5% (2.25–2.35 Å).[19] At room temperature, a solid solution of the α- and β-Pd-H forms at < 0.01 H/Pd[25] which is far below the calculated 0.5 H/Pd[23] needed to achieve reversible voltage-induced switching of the anisotropy, as seen in Fig. 1(b). Therefore, if the formation of the β-Pd-H phase is the rationale behind the irreversible increase in coercivity, it should be resolvable with HR-TEM. To look for evidence of such a transformation in our system, we performed fast Fourier transformations (FFTs) of cross-sectional HR-TEM images (Fig. S3), i.e., the extracted diffractograms [Figs. 2(a) and 2(b)] of a virgin device and a device after several gating cycles. A radial line scan of the diffractograms, shown in Fig. 2(c), shows no discernible shift corresponding to the formation of a β phase, i.e., the virgin and gated reflections overlap. Therefore, it is unlikely that a β-Pd-H phase is present and is the reason for the irreversible increase in coercivity. It is also possible that upon sample preparation of the cross-sectional lamellas, H escapes from the Co/Pd multilayer and causes the spontaneous phase transformation of β-Pd-H back to α-Pd-H. However, identically prepared lamellas were found to reveal the H-induced crystallization of exchange-biased Pd/Co/Pd trilayers.[11] An alternative explanation to the irreversible increase in coercivity may be found in more complex electronic structure effects induced by small quantities of H that become irreversibly trapped in the lattice; however, it is beyond the scope of this work.

Despite the irreversible increase in coercivity of the unloaded state, the voltage-induced loaded state still allows for fully reversible voltage-control of magnetic anisotropy (VCMA) from OOP to IP. In order to maximize the VCMA, we performed a systematic study of the coercivity change and gateability of several heterostructures as a function of Co thickness (X), Pd thickness (Y), and the number of repeating units (N), shown in Fig. 3. Gate voltages of +3 to +5 V for 15–30 s per cycle were used in order to drive the anisotropy IP without causing breakdown of the device.

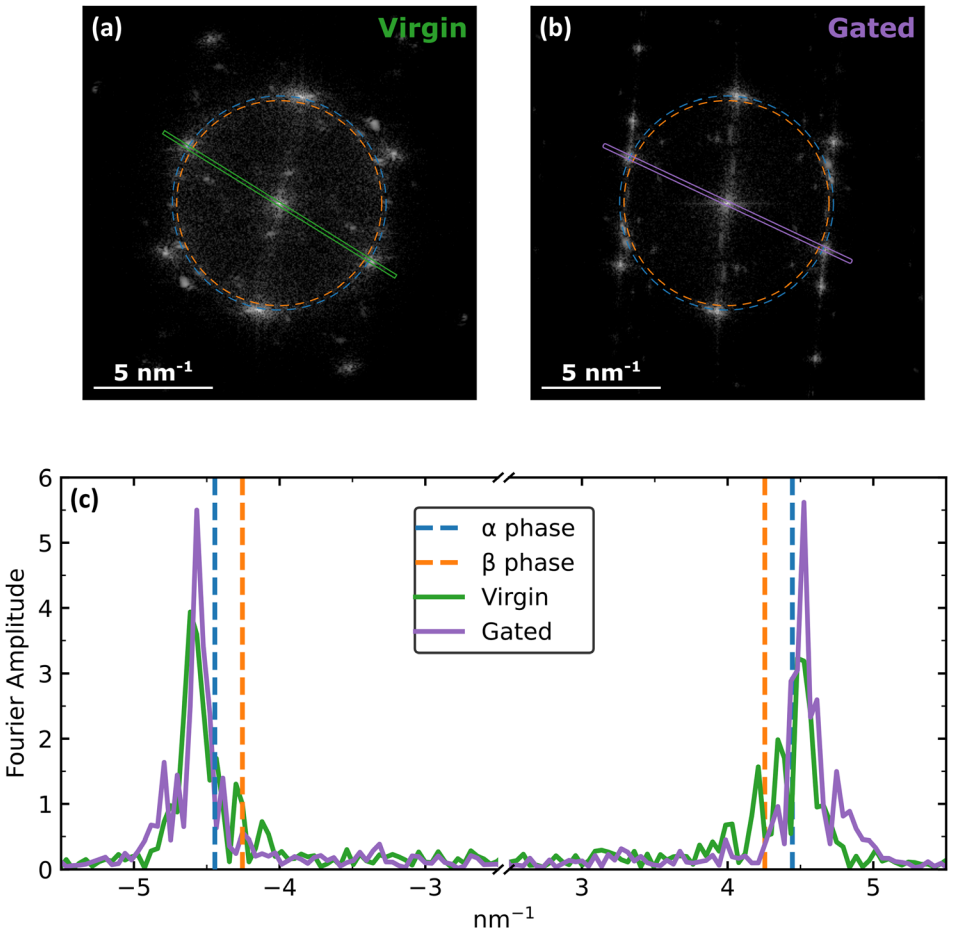

FIG. 2. Diffractograms of the Co/Pd multilayers. Fourier transforms (FTs) of cross-sectional high-resolution transmission electron micrographs of the Co/Pd multilayer region in the heterostructure: Ta(3.5)/Pt(5)/Co(0.2)/[Pd(2)/Co(0.2)]$_{11}$/Pd(6)/GdO$_x$(26)/Au(8) for (a) a virgin device and (b) a device gated for several cycles. (c) Radial line scan of the FTs [region indicated by the diagonal rectangle in (a) and (b)] overlayed and plotted as Fourier amplitude vs distance from the center. The vertical dashed lines represent d_{111} spacing of 2.25 Å, for the α phase, and 2.35 Å, for the β phase, found in Ref. 19.

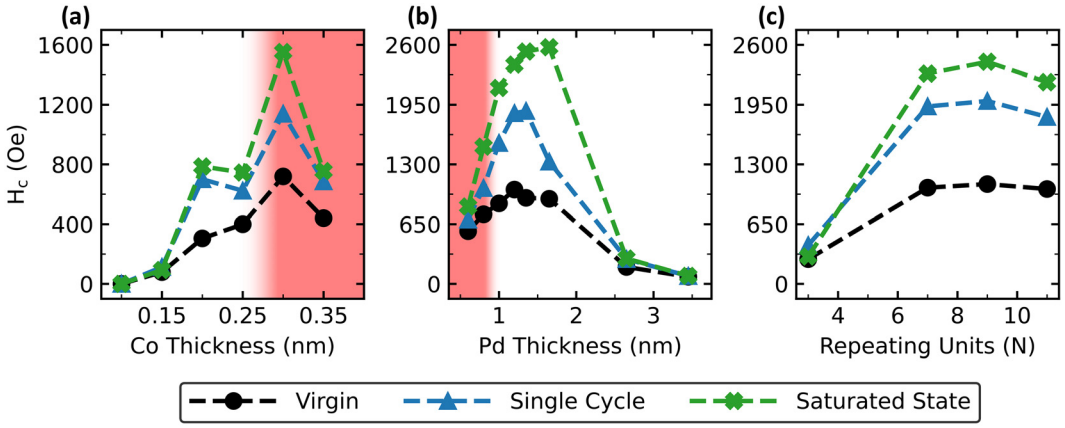

FIG. 3. Irreversible magneto-ionic enhancement of PMA. Coercivity (H_c) in the H-unloaded state for Ta(3.5)/Pt(5)/Co(X)/[Pd(Y)/Co(X)]$_N$/Pd(6)/GdO$_x$(26)/Au(8) in the virgin (ungated) state (black circle), after a single gating cycle (blue triangle), and after several cycles whereupon the irreversible increase in H_c saturates (green cross). (a) H_c as a function of Co thickness. (b) H_c as a function of Pd thickness. (c) H_c as a function of the number of repeating units. The red shaded region indicates thicknesses where the film maintained PMA in the H-loaded state; for the unshaded regions, the films exhibit PMA in the H-unloaded state and IP anisotropy in the H-loaded state.

First, the Co thickness was varied in the heterostructure: Ta(3.5)/Pt(5)/Co(X)/[Pd(1.5)/Co(X)]$_5$/Pd(6)/GdO$_x$(26)/Au(8) (thickness in nm), shown in Fig. 3(a). The coercivity of the virgin state, after one gating cycle, and after several gating cycles was measured using polar MOKE. For low Co thicknesses, the heterostructure can be gated IP, but the coercivity is relatively low. The saturated state coercivity increases with Co thickness up to 3 Å; however, when the Co is too thick ($\geq$ 3 Å), the heterostructure does not go fully IP in the H-loaded state. The heterostructures that did not go IP when a gate voltage was applied are indicated by the red region in Figs. 3(a) and 3(b). Exemplary hysteresis loops of [Co(0.35)/Pd(1.5)]$_5$ in the unloaded and H-loaded states are shown using polar MOKE in Fig. 4(b). It is clear that the anisotropy is reduced in the H-loaded state, but it is not enough to drive the magnetic layer IP. This could be due to an increase of the interfacial anisotropy, with only minimal changes to the volume and shape anisotropy, as the Co thickness increases. This is well known for the Co/Pd multilayer system in the low Co thickness regime.[26]

Similar results are seen for the variation in Pd thickness using the heterostructure: Ta(3.5)/Pt(5)/Co(0.2)/[Pd(Y)/Co(0.2)]$_5$/Pd(6)/GdO$_x$(26)/ Au(8) (thickness in nm), shown in Fig. 3(b). However, the red region occurs when the Pd is too thin ($\leq$ 8 Å), indicating H cannot generate enough variation in the magnetic anisotropy to push the multilayer IP. In addition, the irreversible increase in coercivity is strongly reduced for thick Pd ($\geq$ 2.5 nm). This is likely because the diffusion of H deep into the multilayers is diminished and, therefore, the lower concentration of H at the deep Co/Pd interfaces leads to a smaller change in the interfacial anisotropy.

Finally, using the heterostructure: Ta(3.5)/Pt(5)/Co(0.2)/[Pd(2)/Co(0.2)]$_N$/Pd(6)/GdO$_x$(26)/Au(8) (thickness in nm), the number of repeating units (N) was changed. Beyond N = 7, as seen in Fig. 3(c), there is a broad plateau and gating does not significantly impact the VCMA or the irreversible increase in the coercivity. This is likely due to two competing factors that reach an equilibrium after only a few repeats. By increasing N, the film thickness increases, decreasing the concentration of H that reaches the buried layers. However, the

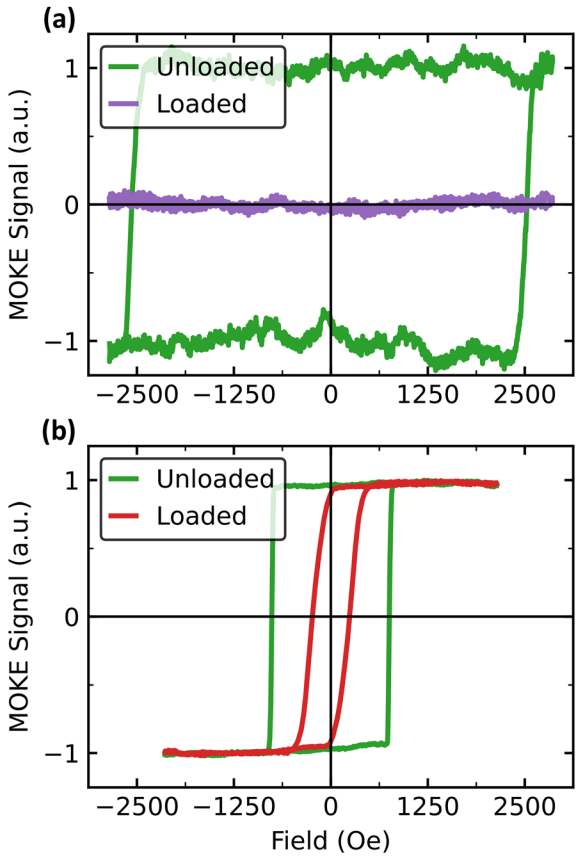

FIG. 4. Voltage-control of magnetic anisotropy. (a) Polar MOKE hysteresis loops of Ta(3.5)/Pt(5)/Co(0.2)/[Pd(1.65)/Co(0.2)]$_5$/Pd(6)/GdO$_x$(26)/Au(8) in the unloaded (green) and H-loaded (purple) state. (b) Polar MOKE hysteresis loops of Ta(3.5)/Pt(5)/Co(0.35)/[Pd(1.5)/Co(0.35)]$_5$/Pd(6)/GdO$_x$(26)/Au(8) in the unloaded (green) and H-loaded (red) state.

number of interfaces that contribute to the interfacial PMA also increases, unlike the case for increasing the Pd thickness, H can still penetrate the uppermost interfaces. If N were to increase significantly more, then the irreversible increase in coercivity would likely decrease as the proportion of H-modified Co/Pd interfaces has decreased relative to the total number of interfaces. The beginnings of this can already be seen in the downturn of the irreversible increase in coercivity at N = 11 in Fig. 3(c).

To maximize the VCMA the optimal range of Co thickness is 2–2.5 Å, Pd thickness is 1.4–1.7 nm, and N is 7–9. Figure 4(a) demonstrates this growth optimization via gated polar MOKE hysteresis loops of the heterostructure: Ta(3.5)/Pt(5)/Co(0.2)/[Pd(1.65)/Co(0.2)]$_5$/Pd(6)/GdO$_x$(26)/Au(8). With only a small bias voltage $V_g = +3$ V, the OOP Co/Pd multilayer goes from $H_c \geq 2500$ Oe to IP in less than 15 s. The efficiency of the VCMA can be calculated using the magneto-electric voltage coefficient $\Delta H_c/|\Delta V|$, giving a value of 858 Oe/V. This is more than an order of magnitude greater than any previous demonstration for a solid-state electrolyte system.[7] Comparing several solid and liquid electrolyte systems, shown in Fig. 5 (with references included in Fig. S4), the VCMA effect achieved here only falls short behind that observed in high-anisotropy $SmCo_5$.[27] However, in that system, the authors did not demonstrate the ability to gate the anisotropy fully in-plane, the device took 1 h to charge, and the gating was performed using a liquid electrochemical cell, all together making this system less practical for on-chip logic or memory.

In conclusion, we demonstrate greater than one order of magnitude improvement in the magneto-electric voltage coefficient by engineering a multilayer heterostructure of Co and Pd. By increasing the number of interfaces, we can dramatically increase the coercivity of the heterostructure without needing to compensate with larger gate voltages. The efficiency of these solid-state devices rivals liquid electrolyte systems, however, have the advantage of faster speeds and easier integration for on-chip logic and memory devices. With scaling the electrolyte thickness and device size down, we anticipate dramatic improvements in device speed, making them an appealing alternative to reduce energy consumption as compared to current-controlled spintronic devices.

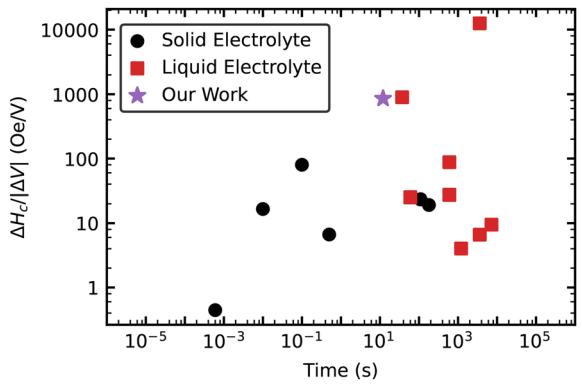

FIG. 5. VCMA efficiency. VCMA efficiency calculated using the magneto-electric voltage coefficients for selected magneto-ionic systems as a function of the device speed. The magneto-electric voltage coefficients are calculated for the largest reversible change in H_c at room temperature. The solid and liquid electrolyte systems are differentiated with black circles and red squares, respectively. References corresponding to each data point are contained in Fig. S4 of the supplementary material.[8–10,13,27–36] Adapted from Ref. 7.

See the supplementary material for the methods, including the polar MOKE measurements and structural characterization, and for the additional figures regarding the coercivity evolution through cycling, HR-TEM, and Fig. 5 with references.

This work was supported by the National Science Foundation (NSF) through the Massachusetts Institute of Technology Materials Research Science and Engineering Center (MRSEC) under Award No. DMR-1419807 and Spintronic Materials for Advanced Information Technologies (SMART) (No. 2018-NE-2861), one of seven centers of nCORE, a Semiconductor Research Corporation program, sponsored by the National Institute of Standards and Technology (NIST). The authors would like to thank Dr. Jonas Zehner for helpful discussions regarding the TEM and Tina Walter for preparing the TEM-lamellas.

AUTHOR DECLARATIONS

Conflict of Interest

The authors have no conflicts to disclose.

Author Contributions

Alexander E Kossak: Conceptualization (lead); Data curation (lead); Formal analysis (lead); Investigation (lead); Methodology (lead); Project administration (lead); Writing – original draft (lead); Writing – review & editing (lead). **Daniel Wolf:** Data curation (equal); Formal analysis (equal); Investigation (equal); Writing – review & editing (equal). **Geoffrey S. D. Beach:** Conceptualization (equal); Funding acquisition (lead); Supervision (lead); Writing – review & editing (equal).

DATA AVAILABILITY

The data that support the findings of this study are available from the corresponding author upon reasonable request.

REFERENCES

[1]S. A. Wolf, D. D. Awschalom, R. A. Buhrman, J. M. Daughton, S. von Molnár, M. L. Roukes, A. Y. Chtchelkanova, and D. M. Treger, "Spintronics: A spin-based electronics vision for the future," Science **294**, 1488–1495 (2001).
[2]J.-G. Zhu, "Magnetoresistive random access memory: the path to competitiveness and scalability," Proc. IEEE **96**, 1786–1798 (2008).
[3]A. Manchon, J. Železny, I. M. Miron, T. Jungwirth, J. Sinova, A. Thiaville, K. Garello, and P. Gambardella, "Current-induced spin-orbit torques in ferromagnetic and antiferromagnetic systems," Rev. Mod. Phys. **91**, 035004 (2019).
[4]F. Matsukura, Y. Tokura, and H. Ohno, "Control of magnetism by electric fields," Nat. Nanotechnol. **10**, 209–220 (2015).
[5]C. Song, B. Cui, F. Li, X. Zhou, and F. Pan, "Recent progress in voltage control of magnetism: Materials, mechanisms, and performance," Prog. Mater. Sci. **87**, 33–82 (2017).
[6]Y. Gu, C. Song, Q. Wang, W. Hu, W. Liu, F. Pan, and Z. Zhang, "Emerging opportunities for voltage-driven magneto-ionic control in ferroic heterostructures," APL Mater. **9**, 040904 (2021).

[7]M. Nichterwitz, S. Honnali, M. Kutuzau, S. Guo, J. Zehner, K. Nielsch, and K. Leistner, "Advances in magneto-ionic materials and perspectives for their application," APL Mater. **9**, 030903 (2021).
[8]U. Bauer, L. Yao, A. J. Tan, P. Agrawal, S. Emori, H. L. Tuller, S. van Dijken, and G. S. D. Beach, "Magneto-ionic control of interfacial magnetism," Nat. Mater. **14**, 174–181 (2015).
[9]A. J. Tan, M. Huang, C. O. Avci, F. Büttner, M. Mann, W. Hu, C. Mazzoli, S. Wilkins, H. L. Tuller, and G. S. D. Beach, "Magneto-ionic control of magnetism using a solid-state proton pump," Nat. Mater. **18**, 35–41 (2019).
[10]K.-Y. Lee, S. Jo, A. J. Tan, M. Huang, D. Choi, J. H. Park, H.-I. Ji, J.-W. Son, J. Chang, G. S. D. Beach, and S. Woo, "Fast magneto-ionic switching of interface anisotropy using yttria-stabilized zirconia gate oxide," Nano Lett. **20**, 3435–3441 (2020).
[11]J. Zehner, D. Wolf, M. U. Hasan, M. Huang, D. Bono, K. Nielsch, K. Leistner, and G. S. D. Beach, "Magnetoionic control of perpendicular exchange bias," Phys. Rev. Mater. **5**, L061401 (2021).
[12]M. Huang, M. U. Hasan, K. Klyukin, D. Zhang, D. Lyu, P. Gargiani, M. Valvidares, S. Sheffels, A. Churikova, F. Büttner, J. Zehner, L. Caretta, K.-Y. Lee, J. Chang, J.-P. Wang, K. Leistner, B. Yildiz, and G. S. D. Beach, "Voltage control of ferrimagnetic order and voltage-assisted writing of ferrimagnetic spin textures," Nat. Nanotechnol. **16**, 981–988 (2021).
[13]H.-B. Li, N. Lu, Q. Zhang, Y. Wang, D. Feng, T. Chen, S. Yang, Z. Duan, Z. Li, Y. Shi, W. Wang, W.-H. Wang, K. Jin, H. Liu, J. Ma, L. Gu, C. Nan, and P. Yu, "Electric-field control of ferromagnetism through oxygen ion gating," Nat. Commun. **8**, 2156 (2017).
[14]S. Manipatruni, D. E. Nikonov, C.-C. Lin, T. A. Gosavi, H. Liu, B. Prasad, Y.-L. Huang, E. Bonturim, R. Ramesh, and I. A. Young, "Scalable energy-efficient magnetoelectric spin–orbit logic," Nature **565**, 35–42 (2019).
[15]X. Li, A. Lee, S. A. Razavi, H. Wu, and K. L. Wang, "Voltage-controlled magnetoelectric memory and logic devices," MRS Bull. **43**, 970–977 (2018).
[16]J. Lee and W. D. Lu, "On-demand reconfiguration of nanomaterials: When electronics meets ionics," Adv. Mater. **30**, 1702770 (2018).
[17]C. Navau and J. Sort, "Exploiting random phenomena in magnetic materials for data security, logics, and neuromorphic computing: Challenges and prospects," APL Mater. **9**, 070903 (2021).
[18]J. Rossmeisl, A. Logadottir, and J. Nørskov, "Electrolysis of water on (oxidized) metal surfaces," Chem. Phys. **319**, 178–184 (2005).
[19]S. Okamoto, O. Kitakami, and Y. Shimada, "Enhancement of magnetic anisotropy of hydrogenated Pd/Co/Pd trilayers," J. Magn. Magn. Mater. **239**, 313–315 (2002).
[20]K. Munbodh, F. A. Perez, C. Keenan, D. Lederman, M. Zhernenkov, and M. R. Fitzsimmons, "Effects of hydrogen/deuterium absorption on the magnetic properties of Co/Pd multilayers," Phys. Rev. B **83**, 094432 (2011).
[21]K. Munbodh, F. A. Perez, and D. Lederman, "Changes in magnetic properties of Co/Pd multilayers induced by hydrogen absorption," J. Appl. Phys. **111**, 123919 (2012).
[22]W.-C. Lin, C.-J. Tsai, B.-Y. Wang, C.-H. Kao, and W.-F. Pong, "Hydrogenation induced reversible modulation of perpendicular magnetic coercivity in Pd/Co/Pd films," Appl. Phys. Lett. **102**, 252404 (2013).
[23]K. Klyukin, G. Beach, and B. Yildiz, "Hydrogen tunes magnetic anisotropy by affecting local hybridization at the interface of a ferromagnet with nonmagnetic metals," Phys. Rev. Mater. **4**, 104416 (2020).
[24]C. Lueng, F. Zighem, D. Faurie, and M. Kostylev, "Ferromagnetic resonance investigation of physical origins of modification of the perpendicular magnetic anisotropy in Pd/Co layered films in the presence of hydrogen gas," J. Appl. Phys. **122**, 163901 (2017).
[25]E. Wicke, H. Brodowsky, and H. Züchner, "Hydrogen in palladium and palladium alloys," in *Hydrogen in Metals II: Application-Oriented Properties* (Springer, Berlin, Heidelberg, 1978), pp. 73–155.
[26]W. R. Bennett, C. D. England, D. C. Person, and C. M. Falco, "Magnetic properties of Pd/Co multilayers," J. Appl. Phys. **69**, 4384–4390 (1991).
[27]X. Ye, H. K. Singh, H. Zhang, H. Geßwein, M. R. Chellali, R. Witte, A. Molinari, K. Skokov, O. Guteisch, H. Hahn, and R. Kruk, "Giant voltage-induced modification of magnetism in micron-scale ferromagnetic metals by hydrogen charging," Nat. Commun. **11**, 4849 (2020).
[28]U. Bauer, S. Emori, and G. S. D. Beach, "Voltage-controlled domain wall traps in ferromagnetic nanowires," Nat. Nanotechnol. **8**, 411–416 (2013).
[29]M. Ameziane, R. Mansell, V. Havu, P. Rinke, and S. van Dijken, "Lithium-ion battery technology for voltage control of perpendicular magnetization," Adv. Funct. Mater. **32**, 2113118 (2022).
[30]L. Reichel, S. Oswald, S. Fähler, L. Schultz, and K. Leistner, "Electrochemically driven variation of magnetic properties in ultrathin CoPt films," J. Appl. Phys. **113**, 143904 (2013).
[31]J. Zehner, I. Soldatov, S. Schneider, R. Heller, N. B. Khojasteh, S. Schiemenz, S. Fähler, K. Nielsch, R. Schäfer, and K. Leistner, "Voltage-controlled deblocking of magnetization reversal in thin films by tunable domainwall interactions and pinning sites," Adv. Electron. Mater. **6**, 2000406 (2020).
[32]C. Navarro-Senent, J. Fornell, E. Isarain-Chávez, A. Quintana, E. Menéndez, M. Foerster, L. Aballe, E. Weschke, J. Nogués, E. Pellicer, and J. Sort, "Large magnetoelectric effects in electrodeposited nanoporous microdisks driven by effective surface charging and magneto-ionics," ACS Appl. Mater. Interfaces **10**, 44897–44905 (2018).
[33]N. Di, J. Kubal, Z. Zeng, J. Greeley, F. Maroun, and P. Allongue, "Influence of controlled surface oxidation on the magnetic anisotropy of Co ultrathin films," Appl. Phys. Lett. **106**, 122405 (2015).
[34]A. Quintana, E. Menéndez, M. O. Liedke, M. Butterling, A. Wagner, V. Sireus, P. Torruella, S. Estradé, F. Peiró, J. Dendooven, C. Detavernier, P. D. Murray, D. A. Gilbert, K. Liu, E. Pellicer, J. Nogues, and J. Sort, "Voltage-controlled ON-OFF ferromagnetism at room temperature in a single metal oxide film," ACS Nano **12**, 10291–10300 (2018).
[35]S. Zhao, Z. Zhou, B. Peng, M. Zhu, M. Feng, Q. Yang, Y. Yan, W. Ren, Z.-G. Ye, Y. Liu, and M. Liu, "Quantitative determination on ionic-liquid-gating control of interfacial magnetism," Adv. Mater. **29**, 1606478 (2017).
[36]X. Zhou, Y. Yan, M. Jiang, B. Cui, F. Pan, and C. Song, "Role of oxygen ion migration in the electrical control of magnetism in Pt/Co/Ni/HfO_2 films," J. Phys. Chem. C **120**, 1633–1639 (2016).